Role of invariant and minimal absorbing areas in chaos synchronization

Gian-Italo Bischi[1] and Laura Gardini[2]
[1]*Istituto di Scienze Economiche, University of Urbino, Urbino, Italy*
[2]*Istituto di Matematica, Facoltà di Economia, University of Parma, Parma, Italy*
and Istituto di Scienze Economiche, University of Urbino, Urbino, Italy
(Received 6 April 1998; revised manuscript received 22 June 1998)

In this paper the method of critical curves, a tool for the study of the global dynamical properties of two-dimensional noninvertible maps, is applied to the study of chaos synchronization and related phenomena of riddling, blowout, and on-off intermittency. A general procedure is suggested in order to obtain the boundary of a particular two-dimensional compact trapping region, called *absorbing area*, containing the one-dimensional chaotic set on which synchronized dynamics occur. The main purpose of the paper is to show that only *invariant* and *minimal* absorbing areas are useful to characterize the global dynamical behavior of the dynamical system when a Milnor attractor with locally riddled basin or a chaotic saddle exists, and may strongly influence the effects of riddling and blowout bifurcations. Some examples are given for a system of two coupled logistic maps, and some practical methods and numerical tricks are suggested in order to ascertain the properties of invariance and minimality of an absorbing area. Some general considerations are given concerning the transition from locally riddled to globally riddled basins, and the role of the absorbing area in the occurrence of such transition is discussed. [S1063-651X(98)11611-2]

PACS number(s): 05.45.+b

I. INTRODUCTION

Dynamical systems with an invariant submanifold of lower dimensionality than the total phase space have commanded increasing interest in the scientific community in recent years. Attracters in Milnor's sense (Ref. [13]), not stable in the Lyapunov sense, appear quite naturally in this context, together with striking phenomena like on-off intermittency and riddled basins, and also interesting kinds of bifurcations like riddling (or bubbling) bifurcations and blowout bifurcations (see, e.g., Refs. [1–5]).

In this paper we study some global properties of two-dimensional discrete dynamical systems, defined by the iteration of a map of the form

$$(x',y')=T(x,y)=(T_1(x,y),T_2(x,y)) \tag{1}$$

that possesses an invariant one-dimensional submanifold S. The very particular feature of the invariance of a submanifold becomes generic if the map T has some symmetry property, a situation that often occurs in applications. The trajectories embedded into S, whose dynamics are governed by the one dimensional restriction of T to S, say $f=T|_S$, are called *synchronized trajectories*. The existence of such one-dimensional dynamics embedded into the two-dimensional phase space of T raises the question, recently investigated by many authors, of whether an attractor A_s of the one-dimensional restriction f is also an attractor of the two-dimensional map T, and in what sense (see, e.g., Ref. [1] and references therein).

Of course, an attractor A_s of the restriction f is stable with respect to perturbations along S, so an answer to the question addressed above can be given through a study of the stability of A_s with respect to perturbations transverse to S (*transverse stability*). Results on transverse stability have been obtained mainly for the case in which the dynamics restricted to the invariant submanifold are chaotic, so that the question of transverse stability is related to the phenomenon of *chaos synchronization*, i.e., trajectories that start outside S and are attracted toward a one-dimensional chaotic attractor $A_s \subseteq S$ (see the Refs. [6,7] or, for more recent results, Refs. [4,5]). A typical example of chaos synchronization, naturally met in many applications, is obtained by coupling two identical one-dimensional chaotic maps (see, e.g., Refs. [8–12]).

In the recent literature, stability statements about chaos synchronization have been given in terms of the *transverse Lyapunov exponents*. The key property is that a chaotic attractor A_s of the restriction $f=T|_S$ includes within itself infinitely many periodic orbits which are unstable in the direction along S, and for the two-dimensional dynamical system the invariant set A_s is asymptotically (Lyapunov) stable, i.e., attracting in the usual topological sense, if all the cycles embedded in it are transversely stable (or, equivalently, if the largest transverse Lyapunov exponent is negative). However, it may occur that some cycles embedded into the chaotic set A_s become transversely repelling even if the *natural transverse Lyapunov exponent* $\Lambda_\perp$ is still negative, due to the presence of many other transversely attracting orbits embedded inside A_s (by the term ''natural Lyapunov exponent,'' we mean the Lyapunov exponent associated to the natural measure, i.e., computed for a typical trajectory on the chaotic attractor A_s). In this case A_s is no longer a Lyapunov attractor, i.e., a two-dimensional neighborhood U of A_s exists such that in any neighborhood $V \subset U$ there are points (really a set of points of positive measure) that exit U after a finite number of iterations, but it continues to be attracting ''on the average'' or, more precisely, it is an attractor in Milnor sense (see Refs. [13,4]), which means that it attracts a positive (Lebesgue) measure set of points of the two-dimensional phase space. The transition from asymptotic sta-

bility to attractivity only in Milnor sense is denoted as a *riddling bifurcation* in Ref. [14] (or a *bubbling bifurcation* in Refs. [11,15,16].

Even if the occurrence of such bifurcations is detected through the study of the transverse Lyapunov exponents, their effects depend on the action of the nonlinearities far from S, that is, on the global properties of the dynamical system. In fact, after the riddling bifurcation two possible scenarios can be observed according to the fate of the trajectories that are locally repelled along (or near) the local unstable manifolds of the transversely repelling cycles:

Situation L: they can be reinjected towards S by the action of the nonlinearities acting far from S, so that the dynamics of such trajectories are characterized by some bursts far from S before synchronizing on it (a very long sequence of such bursts, which can be observed when $\Lambda_\perp$ is close to zero, was called on-off intermittency in Ref. [3]).

Situation G: they may belong to the basin of another attractor, in which case the phenomenon of riddled basins ([2]) is obtained.

Some authors call *local riddling* situation L and, by contrast, *global riddling* situation G (see Refs. [4,17–19]).

When the natural transverse Lyapunov exponent $\Lambda_\perp$ also becomes positive, due to the fact that the transversely unstable periodic orbits embedded into A_s have a greater weight with respect to the transversely attracting ones (see Ref. [5]) a *blowout bifurcation* occurs, after which A_s is no longer a Milnor attractor (it becomes a *chaotic saddle* [20]; also see Ref. [1]). Also the macroscopic effect of a blowout bifurcation is strongly influenced by the behavior of the dynamical system far from the invariant submanifold S: the trajectories starting close to the chaotic saddle may be attracted by some attracting set far from S (that may also be at infinity, i.e., diverging trajectories) or may remain inside some two-dimensional compact set located near or around the chaotic saddle A_s. As noted by many authors (see, e.g., Refs. [3,11,4,10]), the study of transverse Lyapunov exponents, which is based on the linear approximation of the map T around S, says nothing about the fate of the locally repelled trajectories, and the occurrence of the different scenarios described above is determined by the global properties of the map. When Eq. (1) is a noninvertible map, as generally occurs in problems of chaos synchronization, the global dynamical properties can be usefully described by the method of *critical curves* (see Refs. [21–23]), and the reinjection of the locally repelled trajectories can be described in terms of their folding action. [See, e.g., Refs. [22] or [24] for a description of the geometric properties of a noninvertible map related to the folding (or foliation) of its phase space.] This idea was recently proposed in Ref. [25] for the study of symmetric maps arising in game theory, and in [26] for the study of the effects of small asymmetries due to parameters mismatches. In these two papers the geometric properties of the critical curves were used to obtain the boundary of a compact trapping region, called the *absorbing area* following Ref. [22], inside which intermittency and blowout phenomena are confined. In other words, the critical curves are used to bound a compact region of the phase plane that acts as a trapping bounded vessel, inside which the trajectories starting near S are confined.

In a recent paper [19], the notion of absorbing area was introduced in the physical literature for the study of a system of coupled chaotic oscillators, and the authors suggested that the method of critical curves may be used to characterize the global effects of riddling and blowout bifurcations, and that contacts of an absorbing area with basin boundaries may reveal a transition from locally to globally riddling.

The methods used Refs. [26,25,19] are fairly general in the study of the problems related to chaotic synchronization in symmetrically coupled chaotic oscillators. In fact, such systems are generally represented by two-dimensional noninvertible maps, since in this case the restriction of the map to the one-dimensional invariant submanifold of synchronized trajectories may be chaotic. So the critical curves, a powerful tool for the study of global dynamics and bifurcations in noninvertible maps, may be used.

An important question, which was not considered in Ref. [19], is that an absorbing area $\mathcal{A}$, characterized by the property $T(\mathcal{A})\subseteq\mathcal{A}$, may be invariant, i.e., exactly mapped into itself, $T(\mathcal{A})=\mathcal{A}$, or strictly mapped into itself, $T(\mathcal{A})\subset\mathcal{A}$. The purpose of the present paper is to show that only the delimitation of an *invariant absorbing area* is important in order to characterize the global properties which influence the qualitative effects of riddling or blowout bifurcations. Moreover, several invariant absorbing areas may often be observed, one embedded into the other. In these cases the *minimal invariant absorbing area* should be used, where *minimal* means the smallest one including the Milnor attractor on which synchronized dynamics occur.

We give some examples, by using the same system of two coupled one-dimensional maps considered in Ref. [19], in order to illustrate how the boundary of an invariant absorbing area can be obtained by segments of critical curves. Then we address the questions of invariance and minimality properties of an absorbing area, and we show that if either the invariance condition or that of minimality is relaxed, then the absorbing area cannot be used for the purposes stated above. The determination of the minimal invariant absorbing area is not an easy task. So, in order to overcome these difficulties, in Sec. V we suggest the trick of a ''parameter mismatch,'' which turns to be useful in many situations.

Some observations on the transition from local to global riddling are given in Sec. VI. In the recent literature the transition from locally to globally riddling has been considered as a particular bifurcation involving local-global dynamics of the map. Here we argue, by an example, that such transition may occur several times between the riddling and blowout bifurcations, and that the concept of absorbing area may give some help in order to understand such phenomena.

II. CRITICAL CURVES AND THE CONSTRUCTION OF AN ABSORBING AREA

A two-dimensional map $T:(x,y)\to(x',y')$, defined by Eq. (1), is said to be noninvertible if the rank-1 preimages $(x,y)=T^{-1}(x',y')$ of a point $(x',y')\in\mathbb{R}^2$, obtained by solving system (1) with respect to x and y, may be more than one or may not exist. In this case, the plane can be subdivided into regions Z_k, $k\geqslant 0$, whose points have k distinct rank-1 preimages. Generally, as the point (x',y') varies in

the plane $\mathbb{R}^2$, pairs of preimages appear or disappear as it crosses the boundaries separating different regions; hence such boundaries are characterized by the presence of at least two coincident (merging) preimages. This leads to the definition of the critical curves, one of the distinguishing features of noninvertible maps. Following the notations of Refs. [21–23], the *critical set* LC (from the French ''ligne critique'') is defined as the locus of points having two, or more, coincident rank-1 preimages, located on a set (*set of merging preimages*) called LC_{-1}. LC is the two-dimensional generalization of the notion of critical value (when it is a local minimum or maximum value) of a one-dimensional map (this terminology and notation originate from the notion of critical points as it is used in the classical works of Julia and Fatou), and LC_{-1} is the generalization of the notion of the critical point (when it is a local extremum point). Arcs of LC separate regions of the plane characterized by a different number of real rank-1 preimages (see Refs. [21–23]). We also recall that the critical sets of rank k are the images of rank k of LC_{-1} denoted by $LC_{k-1}=T^k(LC_{-1})=T^{k-1}(LC)$, LC_0 being LC.

Points of LC_{-1} in which the map is differentiable are necessarily points where the Jacobian determinant vanishes: in fact in any neighborhood of a point of LC_{-1} there are at least two distinct points which are mapped by T in the same point (near LC); hence the map is not locally invertible in these points. This implies, for a differentiable map T, that

$$LC_{-1}\subseteq J_0=\{(x,y)\in\mathbb{R}^2|\det DT(x,y)=0\}. \tag{2}$$

The condition of a vanishing Jacobian is necessary for differentiable maps, but not sufficient to detect a critical point of LC_{-1} as defined above [i.e., the inclusion in Eq. (2) may be strict]. The notion of critical curve was introduced by Gumowski and Mira in connection with the problem of nonconnected basins and basin bifurcations (see Ref. [21]). Segments of critical curves can be used in order to define trapping regions of the phase plane, called absorbing areas. An *absorbing area* $\mathcal{A}$ is a bounded region of the plane whose boundary is given by critical curve segments (segments of the critical curve LC and its images) such that a neighborhood $U\supset\mathcal{A}$ exists whose point enters $\mathcal{A}$ after a finite number of iterations and then never escape it, since $T(\mathcal{A})\subseteq\mathcal{A}$, i.e., $\mathcal{A}$ is trapping (see Ref. [22], Chap. 4 for more details)

Indeed, in noninvertible maps, boundaries of trapping regions can also be obtained by the union of segments of critical curves and portions of unstable sets of saddle cycles, and in this case we have so-called *absorbing areas of mixed type* (see Ref. [22]). Here we do not enter into such technical details, as in the examples given in this paper only standard absorbing areas (i.e., completely bounded by critical arcs) are used. However, the arguments of the present paper remain substantially unchanged if absorbing areas of mixed type are encountered instead of standard absorbing areas.

Following Refs. [22] or [23], a practical procedure can be outlined in order to obtain the boundary of an absorbing area (although it is difficult to give a general method). Starting from a portion of LC_{-1}, approximately taken in the region occupied by the area of interest, its images by T of increasing rank are computed until a closed region is obtained. When such a region is mapped into itself, then it is an absorbing area $\mathcal{A}$. The length of the initial segment is to be taken, in general, by a trial and error method, although several suggestions are given in the books referred to above. Once an absorbing area $\mathcal{A}$ is found, in order to see if it is invariant or not, the same procedure must be repeated by taking only the portion

$$\gamma=\mathcal{A}\cap LC_{-1} \tag{3}$$

as the starting segment. Then one of the following two cases occurs:

Case I: The union of m iterates of γ (for a suitable m) covers the whole boundary of $\mathcal{A}$, in which case $\mathcal{A}$ is an invariant absorbing area, and

$$\partial\mathcal{A}\subset\bigcup_{k=1}^{m}T^k(\gamma). \tag{4}$$

Case II: No natural m exists such that $\cup_{i=1}^{m}T^i(\gamma)$ covers the whole boundary of $\mathcal{A}$; in which case $\mathcal{A}$ is not invariant but strictly mapped into itself. An invariant absorbing area is obtained by $\cap_{n>0}T^n(\mathcal{A})$ (and may be obtained by a finite number of images of $\mathcal{A}$).

The distinction between the two cases is fundamental in order to consider a contact between the boundary of the absorbing area and some other invariant set (like the boundary of a basin) which generally causes changes for the fate of the trajectories which are locally repelled from the Milnor attractor. For this purpose *only invariant absorbing areas are useful*, because boundary contacts of noninvariant ones generally have no consequences on the invariant sets which are strictly included inside the absorbing areas.

In order to illustrate these concepts let us consider the two-dimensional map F, proposed in Ref. [19], given by a system of coupled logistic maps:

$$F:(x,y)\to(f_a(x)+\varepsilon(y-x),\ f_a(y)+\varepsilon(x-y)), \tag{5}$$

where $f_a(x)=ax(1-x)$ is the standard logistic map, and ε is the coupling parameter. We refer to this map only to give an example, but the arguments and the constructions given below are fairly general.

Map (5) is continuously differentiable in the whole plane $\mathbb{R}^2$, and in this case we have $LC_{-1}=J_0$ [and $LC=F(J_0)$], where J_0 is the locus of points in which the Jacobian vanishes:

$$J_0=\{(x,y)\in\mathbb{R}^2|\det(DF(x,y))=0\}.$$

The equation $\det(DF)=0$ defines an equilateral hyperbola in the plane (x,y); hence LC_{-1} is formed by two branches, denoted by $LC_{-1}^{(a)}$ and $LC_{-1}^{(b)}$ in Fig. 1. This also implies that LC is the union of two branches, denoted by $LC^{(a)}=F(LC_{-1}^{(a)})$ and $LC^{(b)}=F(LC_{-1}^{(b)})$. Branch $LC^{(a)}$ separates region Z_0, whose points have no preimages, from region Z_2, whose points have two distinct rank-1 preimages, and $LC^{(b)}$ separates region Z_2 from region Z_4, whose points have four distinct rank-1 preimages. Notice that $LC_{-1}^{(a)}$ intersects S in the critical point of the restriction f_a, and, consequently, $LC^{(a)}$ intersects S in the point where the restriction

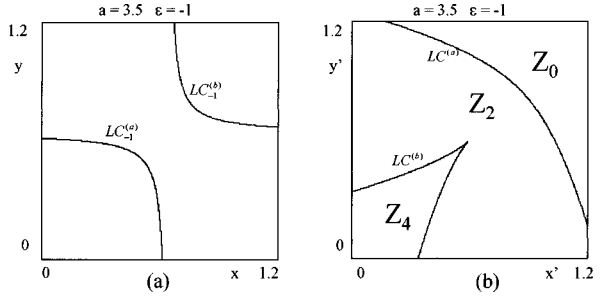

FIG. 1. (a) The set of merging preimages LC_{-1} defined, for map (5), as the locus J_0 of the vanishing Jacobian. (b) Critical curves $LC=F(LC_{-1})$. The regions Z_k represent the set of points having k distinct preimages. The points of $LC^{(a)}$ have two preimages, merging on $LC_{-1}^{(a)}$ the points of $LC^{(b)}$ have four preimages, two of which merge on $LC_{-1}^{(b)}$.

f_a attains its maximum value. Instead the image of the other intersection of LC_{-1} and S is a cusp point of LC.

Following Ref. [19], we now consider fixed values of the parameter a such that a chaotic attractor A_s of the logistic map f_a exists, with an absolutely continuous invariant measure on A_s, and we study the transverse stability of $A_s \subset S$ as the coupling parameter ε varies. We remark that ε is a *normal parameter*, that is, it influences the stability in the transverse directions but it does not affect the dynamics in the invariant diagonal S. Suitable values of the parameter a, at which chaotic intervals for the logistic map exist, are $a=a_i$ for $i=0,1,2,\ldots$, such that, at each value a_i the first homoclinic bifurcation of a cycle of period 2^i occurs, causing the reunion of 2^{i+1} chaotic intervals into 2^i chaotic intervals, merging in the repelling periodic points of the cycle of period 2^i. The 2^i cyclic chaotic intervals give the set A_s on S.

For example, for $a=a_0=3.678\,573\,510\,428\ldots$, A_s is a one-piece chaotic interval, due to the merging of two chaotic intervals into the repelling fixed point different from the origin, which undergoes its first homoclinic bifurcation. In the examples given below we shall also consider $a=a_1=3.592\,572\,184\,106\,97\ldots$, at which A_s is a two-band chaotic set, because a_1 is the parameter value at which the period-2 cycle of the logistic map undergoes the first homoclinic bifurcation, and two cyclic chaotic intervals are obtained by the merging of 4-cyclic chaotic intervals.

III. INVARIANT ABSORBING AREA

Map (5), with $a=a_1$, turns out to be quite useful to give a first example of invariant absorbing area, and will also give us the opportunity to comment, in Sec. VI, on some bifurcations occurring inside it. As stated in Ref. [27], for $a=a_1$ the two-band chaotic set $A_s \subset S$ is an asymptotic (Lyapunov) attractor of the map F for $\varepsilon_1<\varepsilon<\varepsilon_2$, with $\varepsilon_1=-1.464\ldots$ and $\varepsilon_2=-1.156\ldots$ (denoted as interval of strong transverse stability in Ref. [27]). At $\varepsilon=\varepsilon_2$ a riddling bifurcation occurs, due to the loss of transverse stability of a cycle of period 2 embedded inside A_s and, as the coupling parameter ε is further increased, at $\varepsilon=\varepsilon_b$, with $\varepsilon_b=-1.0385\ldots$, a blowout bifurcation occurs, i.e., the natural transverse Lyapunov exponent

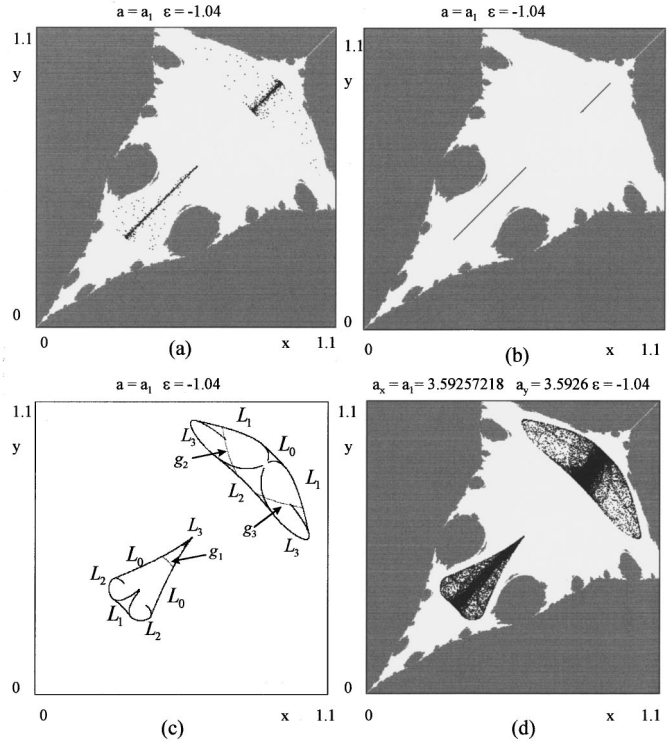

FIG. 2. For $a=a_1$ and $\varepsilon=-1.04$, a chaotic 2-cyclic Milnor (not topological) attractor is embedded into the invariant diagonal. For this set of parameters the natural transverse Lyapunov exponent is $\Lambda_\perp=-0.64\times10^{-2}$. The gray region represents the basin of infinity (divergent trajectories). (a) A generic trajectory starting in the white region synchronizes to the diagonal after several bursts out of it, showing a typical intermittent behavior. (b) The same trajectory as that shown in (a) is represented without the early 2000 iterates. (c) An invariant absorbing area $\mathcal{A}$ around the Milnor attractor is obtained by iterating the *generating arc*, $\gamma=\mathcal{A}\cap LC_{-1}=g_1\cup g_2\cup g_3$, given by the union of three disjoint pieces of J_0, represented by gray arcs. Four iterates of γ, denoted by $L_{k-1}=F^k(\gamma)$, $k=1,\ldots,4$, are represented by black curves. (d) A typical trajectory starting from the diagonal after a parameter mismatch has been introduced, obtained with $a_x=a_1$ in the first equation of Eqs. (9), and $a_y=3.5926$ in the second one.

$$\Lambda_\perp=\lim_{N\to\infty}\sum_{n=1}^{N}\ln|2-2ax_n-2\varepsilon|, \tag{6}$$

where $\{x_n\}$ is a generic trajectory on A_s, becomes positive.

Now let us consider the case $a=a_1$, with the coupling parameter $\varepsilon=-1.04$. From the arguments given above, in such a situation A_s is a Milnor (not asymptotic) attractor. A typical trajectory starting near it synchronizes after a few bursts out of it. This is illustrated in Fig. 2(a), where one of such trajectories is shown. The same trajectory is given in Fig. 2(b), where the early 2000 iterates are not represented. The comparison of these two figures suggests that we have chaotic synchronization after some bursts away from the diagonal, during the transient, represented by the points out of the diagonal in Fig. 2(a). Numerical explorations suggest that a similar behavior is obtained for the generic trajectory starting from the white region of Fig. 2(b), whereas the trajectories starting from the gray region go to infinity. Figure 2(a) suggests that the intermittency phenomena observed during

the transient part of the trajectories are confined inside a compact region of the phase plane, since the trajectories that are locally repelled are folded back toward the diagonal by the global dynamics of the map. In this case an absorbing area $\mathcal{A}$, inside which the Milnor attractor A_s is included, can be easily obtained. Let us consider the set $\gamma=\mathcal{A}\cap LC_{-1}$, ($LC_{-1}=J_0$ for the map F). It is made up of three disjoint arcs, say $\gamma=g_1\cup g_2\cup g_3$ [see Fig. 2(c)], and its first four images by F are necessary to cover the boundary $\partial\mathcal{A}$ of the invariant absorbing area, that is, case I of the procedure described in Sec. II occurs. Moreover, these four images, denoted by $L_{k-1}=F^k(\gamma)$, $k=1,\ldots,4$, in Fig. 2(c), necessarily include several arcs internal to the invariant area $\mathcal{A}$. That is, the boundary of $\mathcal{A}$ is strictly included in the union of the images: $\partial\mathcal{A}\subset\cup_{k=1}^{4}F^k(\gamma)$.

We remark that the same procedure has been followed in Ref. [19], where in order to define the boundary $\partial\mathcal{A}$ of an absorbing area $\mathcal{A}$, the portion of J_0 belonging to $\mathcal{A}$, here called γ, is considered, and a finite number of images $F^k(\gamma)$, $k=1,\ldots,m$, is taken in order to obtain the whole boundary of $\mathcal{A}$. However, Relation (6) given in Ref. [19], i.e., $\partial A=\cup_{k=1}^{m}F^k(\gamma)$, is not correct and, evidently, the inner portions of the critical curves have been canceled to obtain Fig. 4 in Ref. [19].

The images of the critical arcs which are mapped inside the area play a particular role, because these curves represent the ''foldings'' of the Riemann plane under forward iterations of the map, and this is the reason why these inner curves often denote the portions of the region which are more frequently visited by a generic trajectory inside it (many examples that support this statement are given in the literature on noninvertible maps; see, e.g., Ref. [22]).

In the situation shown in Fig. 2, all the trajectories starting inside such an absorbing area are necessarily trapped inside it, and those starting from a neighborhood of $\mathcal{A}$ enter $\mathcal{A}$ after a finite number of iterations and then never escape. The absorbing area behaves as a global vessel for all the trajectories which are repelled away from a local neighborhood of the chaotic saddle A_s.

However, just a few bursts are visible due to the negativity of the natural Lyapunov exponent, which implies that the trajectories synchronize to the Milnor attractor $A_s\subset S$. As will be discussed in Sec. V, a simple method that can be followed to ascertain the existence and shape of an invariant absorbing area consists in the introduction of a small parameter mismatch which breaks the symmetry of the dynamical system, so that the invariance property of S is lost. The result of such a trick is shown in Fig. 2(d): the Milnor attractor A_s embedded into the diagonal is destroyed, and the whole absorbing area appears to be covered by a generic trajectory starting from the white region. From a comparison of Figs. 2(c) and 2(d), it is evident that the portions of $F^k(\gamma)$ internal to $\mathcal{A}$ indicate portions of the absorbing area where the iterated points are more dense.

We take the opportunity to remark that, although for the particular example considered above the relation $\mathcal{A}\cap J_0$ really gives the *generating arc g*, defined as the smallest arc of J_0 whose images include the boundary of an invariant area $\mathcal{A}$ (Ref. [22], Chap. 4), in general the generating arc g may be strictly included in the portion of J_0 belonging to the invariant area. That is,

$$g\subseteq\mathcal{A}\cap J_0, \tag{7}$$

and the strict inclusion in Eq. (7) may occur for two reasons.

(i) The locus J_0 of the vanishing Jacobian, and $\mathcal{A}\cap J_0$ as well, may include a set of points which do not belong to the critical set of rank 0 in the Julia-Fatou sense, denoted by LC_{-1}, to which g must belong. Really Eq. (7) is not the more appropriate notation for the generating arc g, which should be

$$g\subseteq\mathcal{A}\cap LC_{-1}. \tag{8}$$

(ii) Even if the set $\mathcal{A}\cap J_0$ is entirely made up of critical segments belonging to LC_{-1}, it may occur that only a portion of this set is involved in the definition of the boundary of $\mathcal{A}$ because the other portions have images that are always internal to $\mathcal{A}$ (an example is given in Ref. [28], and another example is given below, in Sec. V). In other words, the inclusion given in Eq. (8) also may be strict.

To end this section, we remark that the shape of the absorbing area $\mathcal{A}$ around the Milnor attractor gives us clear information about the consequences of the blowout bifurcation that occurs as the coupling parameter is increased beyond $\varepsilon=\varepsilon_b$. In fact, for values of ε just after the blowout bifurcation, we expect that, the set A_s no longer being attracting in the average (it becomes a chaotic saddle), a generic trajectory will move erratically inside the whole absorbing area. However, in order to make such a prediction we need to know that two important properties hold: the *invariance* and the *minimality* of the absorbing area $\mathcal{A}$. In Sec. IV we give an example of an absorbing area which is not invariant, and in Sec. V we give an example of an invariant absorbing area which is not minimal. In both cases a contact bifurcation of their boundary is not useful to characterize the different scenarios related to riddling or blowout bifurcations of the chaotic set A_s.

IV. NONINVARIANT ABSORBING AREA

To explain the construction of the boundary of an absorbing area better, we consider another example, the one given in Ref. [19], to construct an absorbing area for $a=a_0$ and $\varepsilon=-1.234$. For this set of parameters, considering an arc of LC_{-1}, for example the arc (CD) in Fig. 3(a), and a small portion of the other branch of LC_{-1} including the critical point of the restriction of F on S, nine images by F of these arcs are sufficient to cover the boundary of an absorbing area $\mathcal{A}$. We remark again that such images also include many critical arcs internal to the absorbing area, which are clearly visible in Fig. 3(a). However, this absorbing area is not invariant, because it is impossible to cover the boundary of $\mathcal{A}$ by the images of the set $\gamma=\mathcal{A}\cap J_0$ given by the arc (HK) connecting the points H and K in Fig. 3(a), together with a very small segment on the other branch of LC_{-1}. This is clearly shown in Fig. 3(b): by using the arc $\gamma=\mathcal{A}\cap J_0$, the set $\cup_{k=1}^{9}F^k(\gamma)$ cannot cover the boundary $\partial\mathcal{A}$, nor is the boundary obtained by increasing the number of iterations (i.e., of images of γ).

These arguments prove that the absorbing area $\mathcal{A}$ shown in Fig. 3 of Ref. [19] is not invariant. This implies that such an absorbing area is not useful to characterize the transition

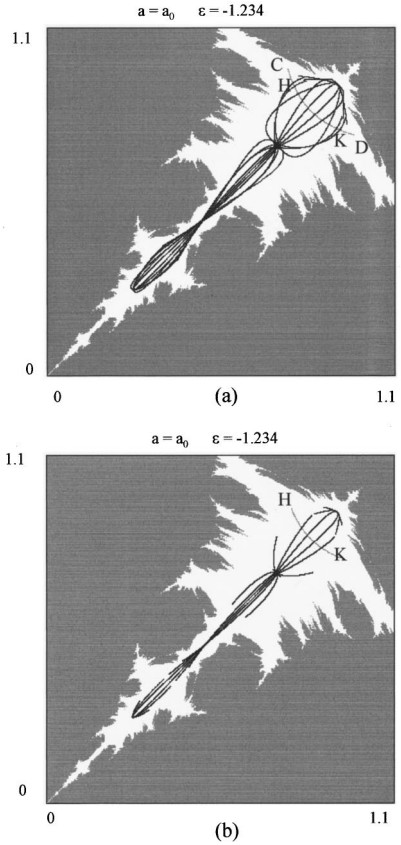

FIG. 3. (a) For $a=a_0$ and $\varepsilon=-1.234$ the union $\cup_{k=1}^{9}F^k(CD)$ of nine iterates of the gray arc (CD) belonging to J_0 covers the boundary $\partial\mathcal{A}$ of an absorbing area $\mathcal{A}$. In this case the arc (CD) is wider than $(HK)=\mathcal{A}\cap J_0$. (b) The critical arcs shown here constitute the set $\cup_{k=1}^{9}F^k(HK)$ which, clearly, cannot cover the boundary of $\mathcal{A}$.

from locally to globally riddling as a consequence of a contact between its boundary with the basin boundary of divergent trajectories (the gray region in Fig. 3 which is really quite close to the absorbing area). For this purpose only invariant absorbing areas must be considered. Moreover, this requirement is still not sufficient to relate the contact bifurcations of the invariant areas to the effects of riddling or blowout bifurcations of the Milnor attractor A_s nested inside it. In fact, only the smallest invariant absorbing area including the weak Milnor attractor, called the *minimal invariant absorbing area*, should be considered. We examine this problem in Sec. V.

V. MINIMAL INVARIANT ABSORBING AREA

The existence of several invariant absorbing areas, embedded one into the other (and all containing the Milnor attractor), is the generic occurrence in two-dimensional noninvertible maps (see, e.g., Refs. [22,23]). Thus a practical procedure to detect the minimal invariant absorbing areas is of primary importance. In previous sections we briefly described a procedure to obtain the boundary of an invariant absorbing area, but how can we ascertain that it is the minimal one? In general this is not an easy task, although some particular (but rather boring) procedures may be given. Here we prefer to suggest a simple trick that can be used with symmetric maps, like the class of maps we are considering, which turns out to be quite useful especially at parameters' values near the blowout bifurcations. In fact, the existence of the invariant diagonal, on which the synchronized dynamics occur, is due to the symmetry of the map F with respect to the diagonal, i.e., it commutes with the operator $S:(x,y)\rightarrow(y,x)$. Such symmetry property is often structurally unstable, i.e., it is lost after an arbitrarily small variation of some parameter (parameter mismatch). A consequence of such symmetry breaking is that the invariance of the diagonal is lost (as well as the Milnor attractor A_s on it). Instead, the existence of a minimal invariant absorbing area $\mathcal{A}$ around A_s is generally structurally stable, i.e., it is persistent under small perturbations of the parameters, even if such perturbations break the symmetry. In fact, the chaotic set $A_s\subset S$ is often embedded into an invariant absorbing area, which is an asymptotic attracting set in the usual Lyapunov (topological) sense, i.e., an invariant set for which a neighborhood U exists such that any point $x\in U$ has the trajectory which satisfies $F^n(x)\in U$ for all $n>N_x$ and $d(P^n(x),\mathcal{A})\rightarrow 0$ as $n\rightarrow\infty$. In order to see which is the minimal absorbing area including the Milnor attractor, we introduce a small parameter mismatch and look at the trajectory obtained by taking an initial condition on the diagonal. If the iterated points are spread in the whole area $\mathcal{A}$, then it is the minimal one.

As an example, let us consider map (5) with $a=a_2=3.574\,804\,938\,759\,2\ldots$ (which corresponds to the homoclinic bifurcation of the logistic map which gives rise to four cyclical chaotic intervals due to the merging by pairs of eight cyclic chaotic intervals). In this case a ''window'' of negative transverse Lyapunov exponent is obtained for $-0.245<\varepsilon<-0.0741$. At $\varepsilon=-0.085$, following the procedure outlined in Sec. II, we consider the two pieces of the curve of merging preimages LC_{-1} denoted by g_1 and g_2 in Fig. 4(a), and after four iterations of the map the boundary of an *invariant* absorbing area $\mathcal{A}_1$ is obtained, which includes the 4-cyclic chaotic Milnor attractor A_s located on the diagonal. Is it the minimal one? Let us consider the generic nonsymmetric map F_m,

$$F_m:(x,y)\rightarrow(f_{a_x}(x)+\varepsilon(y-x),f_{a_y}(y)+\varepsilon(x-y)). \quad (9)$$

After a parameter mismatch, obtained by taking, $a_x=3.574\,804\,938\,759\,2$ in the first equation of F_m and $a_y=3.57$ in the second one, together with the same value $\varepsilon=-0.085$, the trajectory generated by an initial condition on the diagonal is included into an area, say $\mathcal{R}$, which is smaller than $\mathcal{A}_1$ [see Fig. 4(b)]. This means that $\mathcal{A}_1$ is not the minimal invariant absorbing area containing A_s; hence it cannot be used to characterize the effects of riddling or blowout bifurcations. Figure 4(b) also suggests how to determine the desired area around A_s: returning to our symmetric map F, we choose $\gamma=R\cap LC_{-1}$, and repeat the procedure, which now gives the minimal invariant absorbing area $\mathcal{A}_2$. Its boundary $\partial\mathcal{A}_2$ is shown in Fig. 4(c) [and is practically the same as the boundary of the area shown in Fig. 4(b)].

We observe that while the images of both the disjoint pieces of $\gamma=g_1\cup g_2=\mathcal{A}_1\cap LC_{-1}$ are used to cover the boundary $\partial\mathcal{A}_1$, this is not true for the smaller area $\mathcal{A}_2$. In this case $\gamma=\mathcal{A}_2\cap LC_{-1}$ is still made up of two disjoint pieces, but the images of one of them, $\mathcal{A}_2\cap g_2$, are always internal to the invariant absorbing area $\mathcal{A}_2$; hence only im-

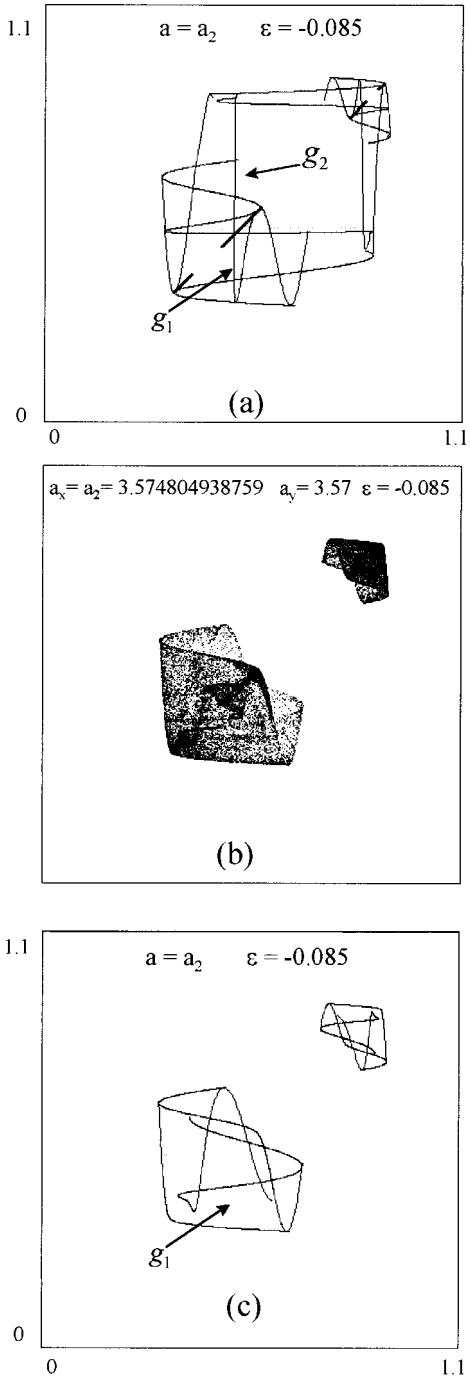

FIG. 4. For $a=a_2$ and $\varepsilon=-0.085$, the natural transverse Lyapunov exponent is $\Lambda_\perp=-0.66\times10^{-2}$. (a) Invariant absorbing area $\mathcal{A}_1$ obtained by four iterations of a generating arc made up of the two portions of LC_{-1}, denoted by g_1 and g_2, and represented by gray color. (b) A trajectory obtained with a parameter mismatch. (c) The minimal invariant absorbing area $\mathcal{A}_2$ obtained by six iterations of the generating arc g_1 made up of only one branch of $\mathcal{A}_2\cap LC_{-1}$.

ages of the other branch, g_1, are involved in the definition of $\partial\mathcal{A}_2$ [see Fig. 4(c)]. This is an example of property (ii) stated in Sec. III, which implies that the strict inclusion holds in Eq. (8), i.e., in this example the generating arc [given by g_1; see Fig. 4(c)] is *strictly included* in $\mathcal{A}_2\cap LC_{-1}$.

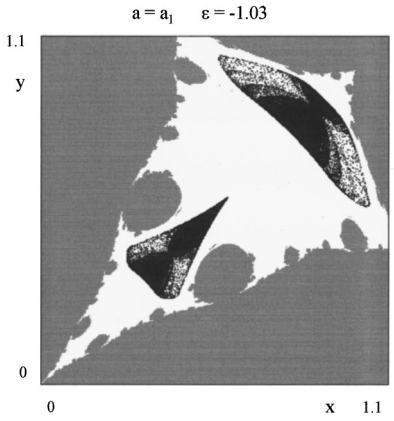

FIG. 5. For $a=a_2$ and $\varepsilon=-0.085$, the natural transverse Lyapunov exponent is $\Lambda_\perp=2.9\times10^{-2}$. A generic trajectory starting in the white region is spread in the whole absorbing area, and shows a typical intermittent behavior.

Another example illustrating how useful the trick suggested above may be was already considered in Sec. III where for $a=a_1$ an invariant area $\mathcal{A}$ was obtained, shown in Fig. 2(c), and a two-band Milnor attractor $\mathcal{A}_s\subset S$, was nested inside $\mathcal{A}$. From Fig. 2(d), obtained after the introduction of a small parameter mismatch, we see that the whole invariant absorbing area appears to be covered by a generic trajectory starting inside $\mathcal{A}_s$, thus giving a clear indication that the absorbing area $\mathcal{A}$ is minimal. We recall that for $a=a_1$ and $\varepsilon_2<\varepsilon<\varepsilon_b$ where $\varepsilon_2=-1.156\ldots$ and $\varepsilon_b=-1.0385\ldots$, the natural transverse Lyapunov exponent $\Lambda_\perp$ is negative. Thus in the case considered in Fig. 2 the value of the parameter ε is quite close to the blowout bifurcation value ε_b. If the boundary of the invariant area does not come into contact with the frontier of its basin of attraction as ε is increased further, we can predict the ''global'' dynamic behavior after the blowout bifurcation. In fact for a value of ε just beyond ε_b we expect that, since the set A_s is no longer attracting on average (it becomes a chaotic saddle), a generic trajectory will move erratically inside the (chaotic) absorbing area. This is shown in Fig. 5, obtained with the same set of parameters as Fig. 4 in Ref. [19].

After the blowout bifurcation, we do not know the ''true'' dynamic behavior of a generic nonsynchronizing trajectory, even if we know that it is bounded inside the minimal invariant absorbing area $\mathcal{A}$. A one-dimensional analog, drawn from the well known behavior of the standard logistic map $x'=ax(1-x)$, may clarify this point. As is well known, after the Feigenbaum point, i.e., for $a\in(3.699,\ldots,4)$, infinitely many periodic ''windows'' are opened by fold bifurcations and are closed by homoclinic bifurcations (see Ref. [29], or the description given in Ref. [30] by the intriguing language of the ''box-within-a-box'' bifurcation structure). Even when the numerical iterations of the logistic map seem to cover some cyclic absorbing interval bounded by critical points, often called ''chaotic intervals,'' we are not sure if the limit set is periodic or chaotic. In the same way, in our two-dimensional noninvertible map, we observe a complex dynamic behavior of the generic trajectory inside the absorbing area, so that a macroscopic dynamical effect is obtained which is often called ''chaotic area'' (or ''chaos in a non strict sense;'' see Ref. [22]) although we are far from a de-

tailed ''microscopic'' knowledge of the dynamic behavior inside the absorbing area. Also in this case the occurrence of saddle-node bifurcations may cause the creation of cycles of different periods, thus giving complex sequences of ''periodic windows'' (or ''boxes'') that are opened and closed through a mechanism similar to the one described for the one-dimensional logistic map. An example of a ''typical'' periodic window is given in Sec. VI.

VI. ROLE OF MINIMAL INVARIANT ABSORBING AREAS IN LOCALLY AND GLOBALLY RIDDLING

From Fig. 5, it is possible to see that the boundary $\partial\mathcal{A}$ of the absorbing area is very close to the boundary of the basin of divergent trajectories (or basin of infinity) $\mathcal{F}$. A further increase of the parameter ε will cause a contact between these two boundaries which marks the destruction of the invariant absorbing area $\mathcal{A}$. As argued in Ref. [19], if such a contact occurs before the blowout bifurcation, i.e., for $\varepsilon_2 < \varepsilon < \varepsilon_b$, it may cause a transition from local to global riddling (with the basin of divergent trajectories), in the sense that before the contact the unstable sets that are locally repelled from the unstable cycles embedded inside A_s are folded back when they reach $\partial\mathcal{A}$, whereas after the contact they may belong to the basin of infinity; i.e., they may diverge (generally after a long transient inside the ''ghost'' of the absorbing area destroyed at the contact).

We stress again that *only when the smallest invariant area, including the Milnor attractor* A_s, has a contact with $\mathcal{F}$ can we state that the basin $\mathcal{B}(A_s)$ becomes globally riddled with the basin of infinity. We notice, however, that this condition is in general only sufficient, and not necessary, for a transition from a locally to a globally riddled basin of A_s. In fact, it may occur, for example, that the basin $\mathcal{B}(A_s)$ becomes globally riddled with the basin of some other attractor existing inside the minimal invariant absorbing area $\mathcal{A}$, such as a stable cycle born via a saddle node bifurcation, *before a contact bifurcation of the boundary of* $\mathcal{A}$ *with the boundary of the basin of divergent trajectories.*

For example, let us consider, again, the situation occurring for $a=a_1$ and $\varepsilon \in (\varepsilon_2, \varepsilon_b)$, i.e., after the riddling and before the blowout bifurcation, when a chaotic 2-cyclic Milnor attractor A_s exists in the invariant diagonal S and is included inside a two-dimensional absorbing area $\mathcal{A}$ like the one shown in Fig. 2(c). The basin of attraction $\mathcal{B}(A_s)$ of the Milnor attractor is at least locally riddled, as in fact the generic trajectory goes away from A_s transversally and may ultimately converge to A_s or not, depending on the global dynamics inside the minimal invariant absorbing area $\mathcal{A}$. In order to understand something of the global behavior inside $\mathcal{A}$, we follow the fate of the transverse unstable set of the repelling 2-cycle embedded inside the chaotic set. We numerically see that for $\varepsilon \in [-1.09\ldots, -1.046\ldots] \subset [\varepsilon_2, \varepsilon_b]$, such an unstable set reaches another attractor (a classical Lyapunov attractor) located out of the diagonal, but inside the minimal invariant absorbing area $\mathcal{A}$ (see Fig. 6). This attractor is created at $\varepsilon = -1.096\ldots$ via a subcritical pitchfork bifurcation, and just after this local bifurcation the transverse unstable manifold of the repelling 2-cycle embedded into A_s converges to the newborn asymptotically stable node of period 4, instead of going back to the diagonal. This

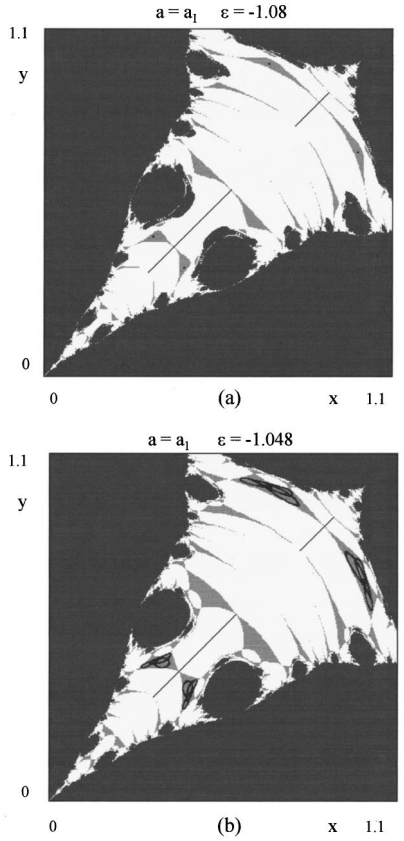

FIG. 6. (a) For $a=a_1$ and $\varepsilon=-1.08$, a stable focus of period 4, of periodic points (x_k, y_k), $k=1,\ldots,4$, with $(x_1, y_1) = (0.4399\ldots, 0.3441\ldots)$, coexists with a 2-cyclic Milnor attractor embedded into the diagonal, characterized by a natural transverse Lyapunov exponent $\Lambda_\perp = -0.119$. The dark-gray points belong to the basin of infinity, the light-gray points to the basin of the cycle out of the diagonal, the white points to the basin of the Milnor attractor. Indeed, the white region is riddled with light-gray points, but this is only visible by zooming in on the figure. The unstable set issuing from the transversely unstable 2-cycle embedded in the Milnor attractor (a repelling node of coordinates 0.868 77 and 0.409 58..., with transverse eigenvalues $\lambda_\perp = -1.37$ and $\lambda_\parallel = -1.72$ along the diagonal) converges to the attracting focus. (b) For $a=a_1$ and $\varepsilon=-1.048$ the chaotic attractor located out of the diagonal is very close to a contact with its basin boundary.

means that the basin of attraction of the newborn attracting cycle has ''tongues'' issuing from the Milnor attractor on the diagonal, and located around the transverse local unstable manifold of the 2-cycle, as well as along the unstable sets issuing from all its preimages of any rank, that are densely distributed along A_s. Only very few of these are visible in Fig. 6, because they become narrower and narrower as preimages of higher and higher rank are considered. This is a typical situation in which the basin of the Milnor attractor A_s is riddled (i.e., globally riddled) with the basin of another attractor out of S, the 4-cycle in our case. In fact, the sufficient conditions stated in Ref. [2] for the occurrence of riddled basins are fulfilled in this case: A_s is a chaotic set with an absolutely continuous invariant measure, the natural transverse Lyapunov exponent $\Gamma_\perp$ is negative, and at least a transversely unstable cycle exists, embedded inside A_s, whose unstable set belongs to the basin of another attractor.

Thus in this case a transition from a locally to a globally riddled basin of A_s may be obtained independently of any contact bifurcations of the minimal invariant absorbing area; it may be simply due to a local bifurcation occurring in the absorbing area $\mathcal{A}$.

We remark, however, that if a similar bifurcation occurs *outside* the minimal absorbing area, i.e., a new attracting cycle is created out of $\mathcal{A}$, no transition to globally riddling occurs, because the locally repelled trajectories starting near the Milnor attractor are not allowed to reach an attractor which is out of the minimal invariant absorbing area (of course this causes a qualitative change in the structure of the basins out of $\mathcal{A}$, but no changes of the dynamics inside $\mathcal{A}$ are obtained).

Taking up our example, the evolution of the attractor out of the diagonal as the parameter ε is increased is rather typical. The stable node becomes a stable focus of period 4, then it loses stability via a Neimark-Hopf bifurcation, after which a more complex attractor is created around it. As ε is further increased, it becomes a larger four-piece chaotic area, and its story ends when it has a contact with the boundary of its basin [see Fig. 6(b), obtained just before such a contact bifurcation]. After this contact bifurcation, called *final bifurcation* in Ref. [22], or *boundary crisis* in Ref. [31], the chaotic attractor out of the diagonal disappears [32] and the scenario of locally riddling may be restored. The chaotic attractor out of the diagonal becomes a chaotic repellor, however, in the region that was occupied by the attractor just destroyed, other attractors may survive, such as stable cycles of very high period with a small basin with fractal structure, so that it is usually difficult to distinguish if $\mathcal{B}(A_s)$ is locally or globally riddled in such a situation. To sum up, the distinction between locally and globally riddling is a very difficult question, since many other ''windows'' in the parameter space may exist in which some stable cycle is created inside the minimal invariant absorbing area via a local bifurcation and then evolves and disappears, through a mechanism similar to the ''box-within-a-box'' bifurcation structure.

We conclude this section with a remark. An interesting statement is given in Ref. [19], concerning the effects of the contact bifurcation that destroys an absorbing area which includes a Milnor attractor: denoting by $\varepsilon^{(a)}$ and $\varepsilon^{(b)}$ the values of riddling bifurcation and of blowout bifurcation, respectively, and by $\varepsilon^{(c)}$ that of contact bifurcation of an absorbing area with the external frontier, different scenarios are predicted depending on $\varepsilon^{(a)}<\varepsilon^{(c)}<\varepsilon^{(b)}$ or $\varepsilon^{(c)}>\varepsilon^{(b)}$. It is now clear that such conclusions are correct only if $\varepsilon^{(c)}$ refers to the *contact bifurcation of the minimal invariant absorbing area, which includes the Milnor attractor* A_s located on the invariant diagonal on which synchronized dynamics occur, and the existence of another attractor inside $\mathcal{A}$ and out of S has been excluded (usually this is not easy to be proved).

We believe that the generic case is the one described in the example shown in Fig. 6, i.e., one or more ''windows'' of parameter intervals (for the coupling parameter) exist at which the basin of A_s is globally riddled with the basin of some other attractor belonging to the minimal invariant absorbing area. Instead, if some other attractor is created out of the minimal invariant absorbing area $\mathcal{A}$, we have qualitative changes in the structure of the basin of A_s in the regions of the phase plane out of $\mathcal{A}$, but no changes can be observed inside $\mathcal{A}$, and in particular no changes concerning the transition from a locally to globally riddled basin. Such changes may be observed only if, due to the variation of some parameters, a contact between the boundary of $\mathcal{A}$ and the boundary of its basin occurs, thus giving the destruction of $\mathcal{A}$ and the consequent possibility that tongues of the basin of the other attractor reach A_s.

Analogously, a contact may occur between the boundary of $\mathcal{A}$ and the boundary of the basin of divergent trajectories. If such a contact occurs in a situation in which a riddled basin already exists inside $\mathcal{A}$, the effect of the contact bifurcation will be that of a further complexity in the riddling, because the basin of attraction of A_s may become riddled with both the basin of infinity and the basin of a bounded attractor out of S.

ACKNOWLEDGMENTS

The work was performed under the activity of the national research project ''Dinamiche non lineari ed applicazioni alle scienze economiche e sociali,'' MURST, Italy, and under the auspices of GNFM, CNR, Italy.

[1] J. Buescu, *Exotic Attractors* (Birkhäuser, Boston, 1997).
[2] J. C. Alexander, J. A. Yorke, Z. You, and I. Kan, Int. J. Bifurcation Chaos Appl. Sci. Eng. **2**, 795 (1992).
[3] E. Ott and J. C. Sommerer, Phys. Lett. A **188**, 39 (1994).
[4] P. Ashwin, J. Buescu, and I. Stewart, Nonlinearity **9**, 703 (1996).
[5] Y. Nagai and Y.-C. Lai, Phys. Rev. E **56**, 4031 (1997).
[6] H. Fujisaka and T. Yamada, Prog. Theor. Phys. **69**, 32 (1983).
[7] L. M. Pecora and T. L. Carrol, Phys. Rev. Lett. **64**, 821 (1990).
[8] A. Ferretti and N. K. Rahman, Chem. Phys. **119**, 275 (1988).
[9] A. Pikovsky and P. Grassberger, J. Phys. A **24**, 4587 (1991).
[10] M. Hasler and Yu. Maistrenko, IEEE Trans. Circuits Syst. I: Fundam. Theory Appl. **44**, 856 (1997).
[11] P. Ashwin, J. Buescu, and I. Stewart, Phys. Lett. A **193**, 126 (1994).
[12] L. Gardini, R. Abraham, R. Record, and D. Fournier-Prunaret, Int. J. Bifurcation Chaos Appl. Sci. Eng. **4**, 145 (1994).
[13] J. Milnor, Commun. Math. Phys. **99**, 177 (1985).
[14] Y. C. Lai and C. Grebogi, Phys. Rev. Lett. **77**, 5047 (1996).
[15] S. C. Venkataramani, B. R. Hunt, E. Ott, D. J. Gauthier, and J. C. Bienfang, Phys. Rev. Lett. **77**, 5361 (1996).
[16] S. C. Venkataramani, B. R. Hunt, and E. Ott, Phys. Rev. E **54**, 1346 (1996).
[17] Yu. Maistrenko, T. Kapitaniak, and P. Szuminski, Phys. Rev. E **56**, 6393 (1997).
[18] Y. C. Lai, C. Grebogi, and J. A. Yorke, Phys. Rev. Lett. **77**, 55 (1996).
[19] Yu. Maistrenko, V. Maistrenko, A. Popovich, and E. Mosekilde, Phys. Rev. Lett. **80**, 1638 (1998).

[20] H. E. Nusse and J. A. Yorke, Ergodyn Th. Dynam. Syst. **11**, 189 (1991).
[21] I. Gumowski and C. Mira, *Dynamique Chaotique* (Cepadues Editions, Toulose, 1980).
[22] C. Mira, L. Gardini, A. Barugola, and J. C. Cathala, *Chaotic Dynamics in Two-Dimensional Noninvertible Maps* (World Scientific, Singapore, 1996).
[23] R. Abraham, L. Gardini, and C. Mira, *Chaos in Discrete Dynamical Systems (A Visual Introduction in Two Dimensions)* (Springer-Verlag, Berlin, 1997).
[24] C. Mira, J.-P. Carcasses, G. Millerioux, and L. Gardini, Int. J. Bifurcation Chaos Appl. Sci. Eng. **6**, 1439 (1996).
[25] G. I. Bischi, L. Stefanini, and L. Gardini, *Mathematics and Computers in Simulations* (Elsevier Science, Amsterdam, 1998), Vol. 44, pp. 559–585 (and presented at the 15th IMACS World Congress, Berlin, August, 1997).
[26] G. I. Bischi, M. Gallegati, and A. Naimzada (unpublished).
[27] Yu. L. Maistrenko, V. L. Maistrenko, A. Popovich, and E. Mosekilde, Phys. Rev. E **57**, 2713 (1998).
[28] L. Gardini, C. Mira, and D. Fournier-Prunaret, in *Iteration Theory*, edited by W. Forg-Rob *et al.* (World Scientific, Singapore, 1996).
[29] P. Collet and J. P. Eckmann, *Iterated Maps on the Interval as Dynamical Systems* (Birkhäuser, Boston, 1980).
[30] C. Mira, *Chaotic Dynamics* (World Scientific, Singapore, 1987).
[31] C. Grebogi, E. Ott, and J. A. Yorke, Physica D **7**, 181 (1983).
[32] I. Gumowski and C. Mira, Comptes Rendus Acad. Sci. Paris Série A **286**, 427 (1978).